PROCEEDINGS OF SCIENCE

ITS3, the ALICE Vertex Detector for LHC Run 4

Filip Krizek[†,*]

[a] *Nuclear Physics Institute of the Czech Academy of Sciences, Hlavni 130, Husinec–Rez, Czechia*

E-mail: krizek@ujf.cas.cz

During LHC Long Shutdown 3 (2026–2028), the ALICE Collaboration plans to upgrade the innermost layers of the current Inner Tracking System detector (ITS) with a novel vertex detector ITS3. The concept of this new vertex detector is based on ultra-thin (< 50 μm), wafer-scale (up to about 10×26 cm^2 large) Monolithic Active Pixel Sensors (MAPS) that are fabricated using the 65 nm CMOS process. Such sensors can be bent to radii as small as 18 mm and can be utilized to construct truly cylindrical-detector shells with an unprecedently low material budget, 0.05% X_0 per layer only. The development of this detector includes a number of cutting-edge R&D efforts, including the qualification of MAPS in 65 nm, the development of wafer-scale stitched MAPS, the concept of bent MAPS, ultra-light mechanics based on carbon foam supports, and air cooling. This contribution provides an overview of the ALICE ITS3 detector and of the R&D achievements, including: the validation of the 65 nm technology for particle tracking and radiation hardness, the achievements in terms of bending and flexibility, the integration of wafer-scale silicon detectors, and the production of the first MOnolithic Stitched Sensor (MOSS).

The 32nd International Workshop on Vertex Detectors (VERTEX2023)
16-20 October 2023
Sestri Levante, Genova, Italy

*Speaker
†On behalf of the ALICE Collaboration

https://pos.sissa.it/

PoS(VERTEX2023)033

1. Introduction

Before the LHC Run3, the ALICE experiment at CERN underwent a major upgrade, which allows the collaboration to perform precise measurements of low-p_{T} open-heavy-flavor hadrons, low-mass dielectrons, and light nuclei, antinuclei, and hypernuclei. A key part of the upgrade was the installation of a new silicon tracker called Inner Tracking System (ITS) [1]. For the LHC Run 4, the collaboration is preparing a follow-up upgrade that will replace the inner barrel of the ITS by a detector with a new design [2].

The inner barrel of the present ITS consists of three layers of MAPS sensors produced in 180 nm CMOS process. For precise reconstruction of low-p_{T}, open-heavy-flavor hadrons, it is important that the first ITS layer is as close as possible to the interaction vertex and that the detector has a low material budget. The first layer of the present inner barrel is at a radius of 22 mm from the beam axis and the material budget of the ITS inner barrel is 0.35% X_0/layer. This material budget consists mainly of passive structures such as a carbon support frame, a flexible printed circuit, and water cooling. The silicon sensors represent $1/7^{\mathrm{th}}$ of the material budget only. The new inner barrel design therefore plans to remove these passive structures. To remove the water cooling, power consumption needs to be reduced such that the detector can be cooled by airflow. In addition, the sensor cooling would also benefit from moving the sensor periphery including the serial link to the edge of the sensor. The sensor periphery produces most of the heat and its location at the edge allows cooling by a radiator. The circuit board can be replaced by integration of power and data buses on the chip. Finally, the amount of material required for mechanical support can be significantly reduced by utilizing the stiffness of large-sized, bent silicon wafers.

The new inner barrel, called ITS3, will consist of 6 large scale, bent MAPS sensors that will be arranged in 3 layers, see Fig. 1. The sensors will be as large as 26×9 cm^2 and they will be thinned to less than 50 µm so that they can be shaped into a half-cylinder. The radius of the first layer will be 18 mm only. Mechanical support of the sensors will be provided by carbon foam spacers. This design enables to keep the material budget at the level of 0.05% X_0/layer.

The large MAPS sensors will be the first ever high-energy-physics silicon sensors fabricated on 300-mm wafers using the 65-nm CMOS process with one-dimensional stitching. The spatial resolution of the sensors is required to be about 5 µm and they should be radiation hard at least up to 10 kGy and 10^{13} 1 MeV n$_{\mathrm{eq}}$ cm^{-2}.

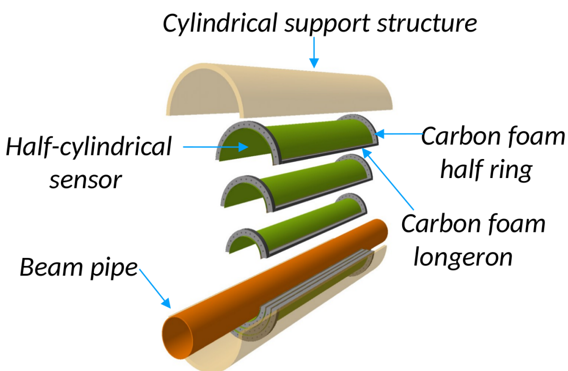

Figure 1: Layout of the ITS3 detector.

This design improves the pointing resolution in the plane transverse to the beam direction by a factor of 2 and it also increases reconstruction efficiency for tracks with transverse momentum less than 200 MeV/c [2]. This will have a positive impact on heavy-flavor baryon measurements which can be illustrated by a projection for the challenging reconstruction of Λ_c^+ baryon from its decay to $\mathrm{p\,K^-\,\pi^+}$ in 0–10% central Pb–Pb collisions at $\sqrt{s_{\mathrm{NN}}}$ = 5.5 TeV. The significance of the Λ_c^+ peak will improve by a factor of 3 to 4 w.r.t. the present ITS2. For more details see Ref. [3], where one can find also projections for other measurements.

2. Current status of ITS3 R&D

The R&D of ITS3 pursues several lines in parallel. The ongoing activities encompass sensor design, sensor prototype characterization, detector mechanics, and air cooling. The timeline for the R&D of ITS3 sensors is shown in Table 1. The first years are dedicated to four successive stages of ITS3 sensor development. In the first stage, called Multi Layer Reticle 1 (MLR1), different variants of digital and analog pixel test structures were characterized in terms of charge collection, detection efficiency for minimum-ionizing-particles, fake-hit rate, and radiation hardness. The recent paper [4] reports on performance of the digital pixel test structure, which features in-pixel front-end that performs amplification, discrimination, and digitization of the charge collected by the n-well diode in each pixel. The reported results illustrate that the digital test structure is radiation hard enough to sustain the radiation load that is expected for ITS3. Note that the observed good radiation hardness of the tested structures is also largely due to the new pixel design, which introduced a low-dose n-type implant with a gap [5]. This implant allows full depletion of the sensitive volume, increases charge collection speed, and thus reduces charge sharing between neighboring pixels.

Table 1: Timeline of the ITS3 R&D project showing the periods dedicated to characterization of successive sensor prototypes (MLR1, ER1, ER2, ER3), final detector assembly and commissioning, and operation in Run 4. See text for more details.

2021	2022	2023	2024	2025	2026 – 2028	2029 – 2032
MLR1		ER1	ER2	ER3	Detector assembly and commissioning	Run 4

The MLR1 stage is followed by three Engineering Round stages designated ER1, ER2, and ER3. These are being devoted to investigating the stitching process, selecting and testing the final sensor design, and fabricating the final sensors, respectively. In the ER1, it is important to determine the production yield of working sensors. Further, the sensors need to be characterized in terms of power consumption and temperature distribution on their surface, and it has to be verified that the sensors can be operated and read out via the stitched backbones.

During the ER1, two stitched-sensor variants are investigated, they are called MOnolithic Stitched Sensor (MOSS), and MOnolithic Stitched sensor with Timing (MOST). The MOSS chip is 26 cm long and 1.4 cm wide. The sensor consists of ten repeated sensor units (RSU), which are having their power and data busses interconnected by means of stitched metal traces with the right and left sensor endcaps, see Fig. 2. Each RSU consists of a top and a bottom half-unit, which are further segmented into 4 regions. The top and a bottom half-units have different pixel pitch, in order to test two designs of pixel architecture. Each region in the top half-unit contains 256×256 pixels, while the regions in the bottom half-unit have 320×320 pixels. Thus, the total number of pixels hosted by the whole MOSS sensor is 6.72×10^6.

The MOSS sensor is operated by a setup that is shown in Fig. 3. The MOSS sensor is mounted on a carrier card, which provides access to all features of the chip via five 560-pin connectors located along its perimeter. Four of them are used to control four quadrants of the MOSS sensor. Each quadrant contains five independently operable half-units. The fifth connector, which is on the short side of the carrier card, operates the upper half-units and lower half-units via the stitched backbone. These connectors are used to plug five proximity cards, which provide power supply, control, and readout. Each of the proximity boards is steered with an automation and readout module that interfaces the sensor control and readout with a computer.

Let us now focus on the ITS3 mechanics and related R&D. The large MAPS sensors can be bent into a half-cylinder shape of a given radius using a mandrel as illustrated in Fig. 4. The shape of the bent sensor is then fixed by gluing a carbon-foam half-ring and a carbon-foam longeron, see Fig. 1. Those are made of two kinds of carbon foam. The carbon-foam half-rings are made of carbon foam with higher density (≈ 0.2 kg dm^{-3}) and higher thermal conductivity (≥ 17 W m^{-1}K^{-1}) because most of the heat production on the sensor will be at its perimeter. Therefore, in addition to providing mechanical support, these half-rings act as a heat sink. On the other hand, the longerons are made of low-density carbon foam (≈ 0.045 kg dm^{-3}) with low thermal conductivity (≥ 0.033 W m^{-1}K^{-1}), as no significant amount of heat is expected to be generated along the sensor matrix.

The dummy half-cylinder sensors are used to construct ITS3 breadboard models shown in Fig. 4. These breadboard models are equipped with an air distributor and heating and they are tested in a wind tunnel for their thermal properties and mechanical stability. For the expected conditions, when the surface power densities at the sensor matrix are 25 mW/cm^2 and 1000 mW/cm^2 in the end-cap regions, it has been shown that an airflow of 8 m s^{-1} provides sufficient cooling of the sensors and can keep their temperature below 30 °C [6]. The performance above will remain even for higher power dissipation (< 50 mW/cm^2 on average) in the matrix region.

Mechanical vibrations induced by flowing air are measured using a confocal sensor. The observed displacements stay below 0.5 μm and are below the spatial resolution of the sensor. It is expected that the amplitude of the observed vibrations can be further decreased after optimization of the holes in the carbon-foam half-rings.

Finally, let us also mention the progress in the R&D area dealing with the characterization of bent silicon sensors. A dedicated μITS3 setup was built for this purpose, see Fig. 5. The setup consists of six 50 μm thick ALPIDE monolithic active pixel sensors [7] bent to the radii of the ITS3 layers. The sensors were characterized in terms of detection efficiency and spatial resolution for minimum ionizing particles. The left plot in Fig. 5 shows detection inefficiency versus charged threshold. Let us point out that at the nominal working point, which is located at the 100-electron threshold, the sensors provide detection efficiency better than 99% which is compatible with a flat ALPIDE sensor. The efficiency does not depend on bending radius. Likewise it was found that the bending does not affect spatial resolution. A similar measurement done with a single bent ALPIDE sensor was published in Ref. [8].

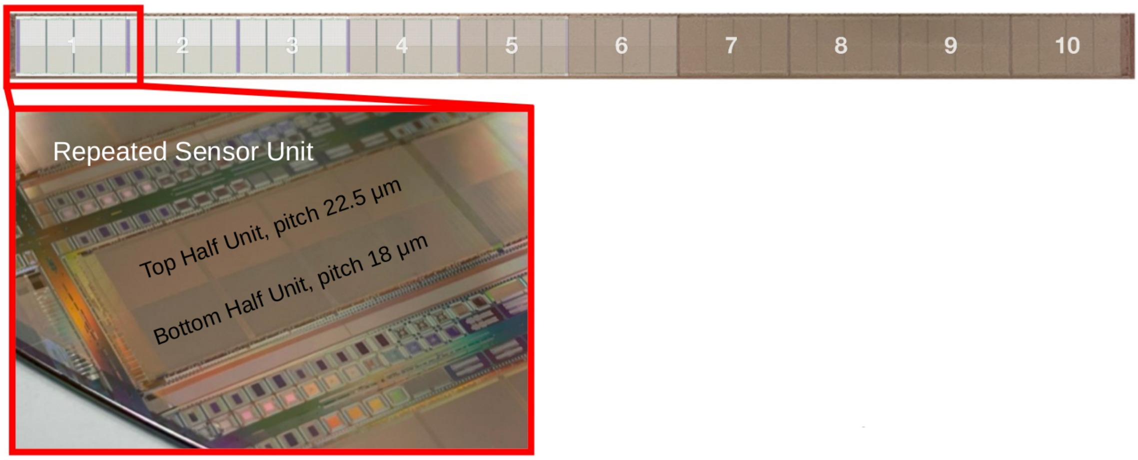

Figure 2: MOSS sensor.

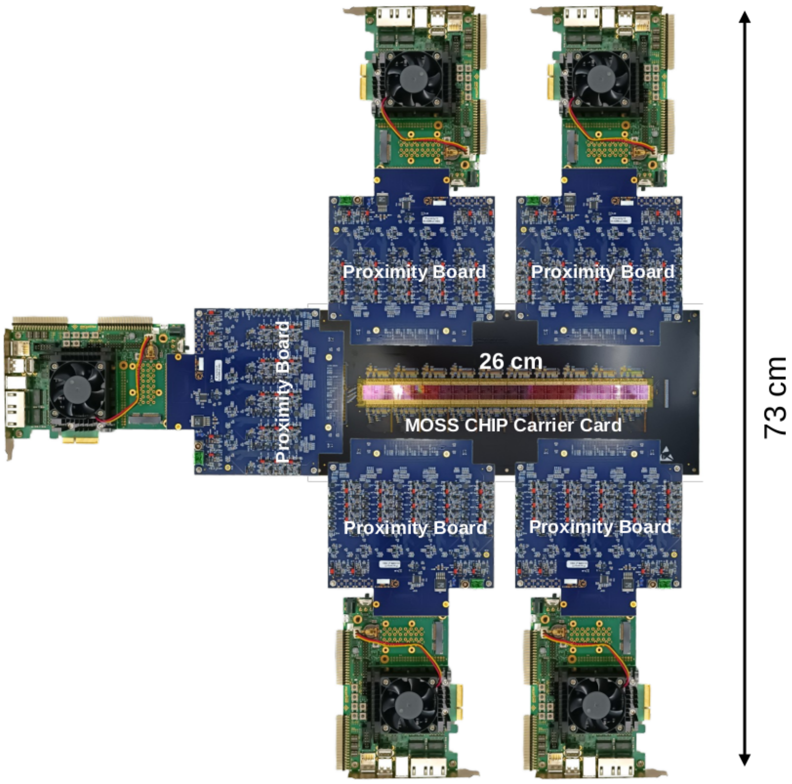

Figure 3: MOSS chip test setup.

Figure 4: Left: A dummy 50 μm thick silicon sensor bent to a radius 19 mm on a mandrel. Middle: Breadboard model. Right: Breadboard model dressed for a test in the wind tunnel with an air distributor and heater.

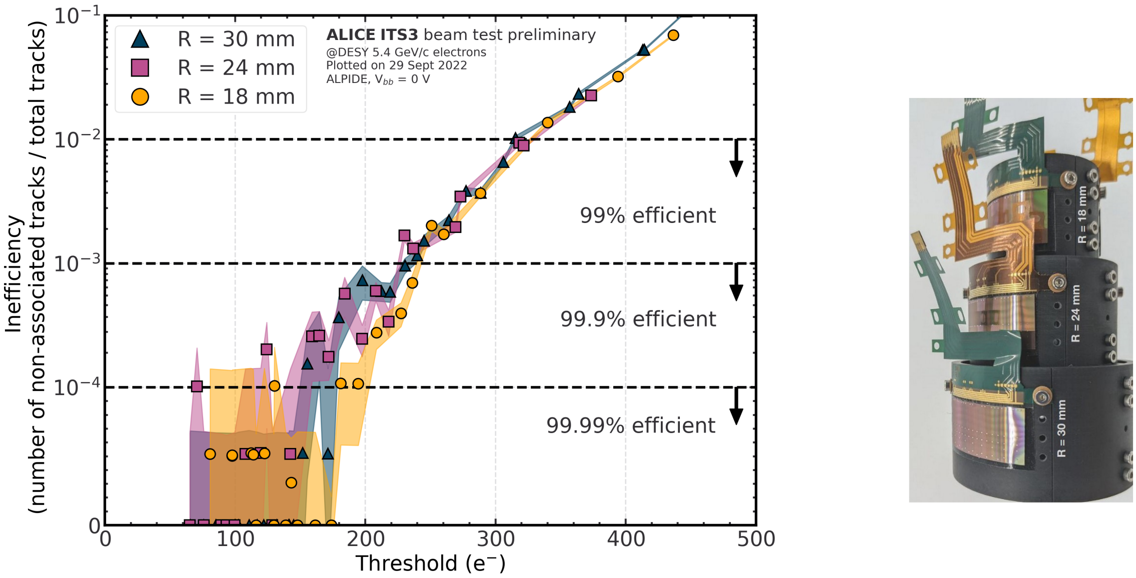

Figure 5: Left: Inefficiency to register a minimum ionizing particle by a bent ALPIDE sensor versus imposed charge threshold. Right: μITS3 setup.

3. Summary

The ALICE Collaboration plans to upgrade the inner barrel of the ITS tracker with a novel concept of silicon detector that will be based on large-scale, bent monolithic active pixel sensors produced by stitching. The R&D of this detector is ongoing. So far it has been shown that it is possible to bent large-scale silicon sensors to curvatures as small as 18 mm. It has been demonstrated the bent sensors have the same properties as flat sensors. and it has been found that the current silicon sensor prototypes are radiation hard enough and meet the limits for ITS3. At present, the R&D focuses on characterization of stitched sensors and investigates air cooling. All this development paves way to thin, low-power sensors for the future ALICE 3 detector [9].

F. Krizek acknowledges support by the Ministry of Education, Youth and Sports of the Czech Republic project LM2023040.

References

[1] ALICE Collaboration, *Technical Design Report for the Upgrade of the ALICE Inner Tracking System*, J. Phys. G 41 (2014) 087002.

[2] ALICE Collaboration, *Expression of Interest for an ALICE ITS Upgrade in LS3*, ALICE-PUBLIC-2018-013.

[3] ALICE Collaboration, *Upgrade of the ALICE Inner Tracking System during LS3: study of physics performance*, ALICE-PUBLIC-2023-002.

[4] G. Aglieri Rinella et al., *Digital Pixel Test Structures implemented in a 65 nm CMOS process*, Nucl. Instr. Meth. Phys. Res. A 1056 (2023) 168589.

[5] M. Munker et al., *Simulations of CMOS pixel sensors with a small collection electrode, improved for a faster charge collection and increased radiation tolerance*, JINST 14 (2019) C05013.

[6] ALICE Collaboration, *Technical Design Report for the ALICE Inner Tracking System 3 – ITS3, A bent wafer-scale monolithic pixel detector*, CERN-LHCC-2024-003/ALICE-TDR-021.

[7] G. Aglieri Rinella et al., *The ALPIDE pixel sensor chip for the upgrade of the ALICE Inner Tracking System*, Nucl. Instr. Meth. Phys. Res. A 845 (2017) 583.

[8] ALICE ITS project, *First demonstration of in-beam performance of bent Monolithic Active Pixel Sensors*, Nucl. Instr. Meth. Phys. Res. A 1028 (2022) 166280.

[9] ALICE Collaboration, *Letter of intent for ALICE 3: A next generation heavy-ion experiment at the LHC*, CERN-LHCC-2022-009.